Altered DNA methylation pattern characterizes the peripheral immune cells of patients with autoimmune hepatitis

Kalliopi Zachou[1,2*], Pinelopi Arvaniti[1*], Aggeliki Lyberopoulou[1], Eirini Sevdali[3], Matthaios Speletas[3], Maria Ioannou[4], George K. Koukoulis[4], Yves Renaudineau[5,6**], George N. Dalekos[1,2**]

*These authors contributed equally to this work

**These authors contributed equally to this work as senior authors

[1]Department of Medicine and Research Laboratory of Internal Medicine, National Expertise Center of Greece in Autoimmune Liver Diseases, General University Hospital of Larissa, 41110 Larissa, Greece; [2]Institute of Internal Medicine and Hepatology, 41447 Larissa, Greece; [3]Department of Immunology and Histocompatibility, Faculty of Medicine, School of Health Sciences, University of Thessaly, Larissa, Greece; [4]Department of Pathology, Faculty of Medicine, School of Health Sciences, University of Thessaly, Larissa, Greece; [5]INSERN U1291, CNR U5051, University Toulouse III, Toulouse Institute for infectious and inflammatory diseases, Toulouse, France; [6]Department of Immunology, Purpan University Hospital Toulouse, Toulouse, France

All correspondence and reprint requests to:

George N. Dalekos, MD, PhD

Professor of Medicine

Head, Department of Medicine and Research Laboratory of Internal Medicine

National Expertise Center of Greece in Autoimmune Liver Diseases

General University Hospital of Larissa, 41110 Larissa, Greece

Tel: ++30-241-350-2285; Fax: ++30-241-350-1557

e-mail: georgedalekos@gmail.com

Key words: Autoimmune hepatitis, epigenetics, DNA methylation, DNA-methyltransferases, ten-eleven translocation enzymes, epigenome wide association studies.

Word count: 3998

Tables and Figures: 8

Conflict of interest: none

Financial support: This research project was supported in part by a research grant from the Hellenic Association for the Study of the Liver (HASL) and the Research Committee of the University of Thessaly (No. 2466). P. Arvaniti was also supported by a research grant for rare diseases by the Federation for the Development of Internal Medicine in Europe (FDIME).

Author contributions: Study concept and design: Kalliopi Zachou, George N Dalekos, Yves Renaudineau. Acquisition of research data: Pinelopi Arvaniti, Aggeliki Lyberopoulou, Eirini Sevdali, Maria Ioannou. Analysis and interpretation of data: Pinelopi Arvaniti, Kalliopi Zachou, George N Dalekos, Yves Renaudineau, Matthaios Speletas, Maria Ioannou, George K Koukoulis. Drafting of the manuscript: Pinelopi Arvaniti, Kalliopi Zachou, George N Dalekos, Yves Renaudineau. Critical revision and editing of the manuscript: Kalliopi Zachou, George N Dalekos, Yves Renaudineau, Matthaios Speletas, George K Koukoulis.

NOTE: Preliminary results of this project have been presented as an abstract in the 18th European Congress of Internal Medicine, Lisbon 29-31 August, 2019, the 18th Hellenic Congress of Hepatology, Athens 11-13 September, 2020 and the 19th Hellenic Congress of Hepatology, 6-9 May 2021.

Abstract

Objective: AIH is a chronic liver disease of unknown aetiology with favourable response to immunosuppression. Little is known about the impact of methylation modifications on disease pathogenesis.

Design: 10 patients with AIH at diagnosis (time-point 1; tp1), 9 with primary biliary cholangitis (PBC) and 10 healthy controls (HC) were investigated. 8/10 AIH patients were also investigated following biochemical remission (time-point 2; tp2). Peripheral CD19(+)- and CD4(+)-cells were isolated to study global DNA methylation ($5^{m}C$)/hydroxymethylation ($5^{hm}C$) by ELISA and mRNA of DNA methylation (DNMT1/3A/3B)/hydroxymethylation enzymes (TET1/2/3) by quantitative RT-PCR. Epigenome wide association study (EWAS) was performed in CD4(+)-cells (Illumina HumanMethylation 850K array) in AIH and HC. Differences in total $5^{m}C/5^{hm}C$ state between AIH-tp1 and HC were also assessed by immunohistochemistry (IHC) on paraffin embedded liver sections.

Results: Reduced TET1 and increased DNMT3A mRNA levels characterized CD19(+) and CD4(+) lymphocytes from AIH-tp1 patients compared to HC and PBC respectively, without affecting global DNA $5^{m}C/5^{hm}C$. In AIH-tp1, CD4(+) DNMT3A expression was negatively correlated with serum IgG ($p=0.03$). In remission (AIH-tp2), DNMT3A decreased in both CD19(+) and CD4(+)-cells ($p=0.02$, $p=0.03$, respectively). EWAS in CD4(+)-cells from AIH patients confirmed important modifications in genes implicated in immune responses (HLA-DP, TNF, lnRNAs and CD86). IHC confirmed increased $5^{hm}C$ staining of periportal infiltrating lymphocytes in AIH-tp1.

Conclusion: Altered expression of TET1 and DNMT3A, characterizes peripheral immune cells in AIH. DNMT3A is associated with disease activity and decreased following therapeutic response. Gene specific DNA methylation modifications affect immunologic pathways that may play an important role in AIH pathogenesis.

Words: 249

Summary box

What is already known?

Autoimmune hepatitis (AIH) is a non-resolving chronic liver disease of unknown aetiology and favourable response to immunosuppression. Since the interplay between the genetic background and the environment seems to be fundamental for AIH pathogenesis, epigenetic modifications may be of particular importance.

What are the new findings?

We found characteristic alterations of DNA methylation in peripheral immune cells of AIH patients, which were associated with disease activity and modified by immunosuppressive treatment.

How might it impact on clinical practice in the foreseeable future?

These results provide the first evidence that epigenetics play a role in AIH pathogenesis, which may have therapeutic implications for the management of the disease.

Introduction

Autoimmune hepatitis (AIH) is a chronic liver disease characterized by hypergammaglobulinaemia, autoantibodies, interface hepatitis and favourable response to immunosuppression (1–6). Although its aetiology remains unknown, the interaction between genetic and environmental factors seems fundamental in AIH pathogenesis (2,3,6).

Genetic predisposition to AIH has been linked to genes within the human leucocyte antigen (HLA) region, particularly with the allelic variants *HLA DRB1*0301* and *DRB1*0401* of DRB1, while weaker associations have been found with non-HLA genes (7,8). However, *HLA DRB1*0301* and *DRB1*0401* genotypes associations occur in only 51-55% of patients among different ethnicities, age groups and geographic regions, indicating that additional factors, such as epigenetic changes, could contribute to its pathogenesis (7,9).

Epigenetic modifications, consisting of DNA methylation, histone adjustment and micro-RNAs (miRNAs), influence gene expression without altering the DNA sequence. In eukaryotic cells, DNA methylation represents the central epigenetic process and refers to the methylation of carbon 5 of cytosine ($5^{m}C$) at the cytosine-phosphate-guanine dinucleotides (CpGs) by DNA methyl-transferases (DNMT1,3A,3B) (10-12). The latter is counterbalanced by an active DNA demethylation process comprising of the oxidization of $5^{m}C$ into 5-hydroxymethylcytosine ($5^{hm}C$) by Ten Eleven Translocation (TET1,2,3) deoxygenases (13).

Epigenetic studies have been performed mainly in liver fibrosis, non-alcoholic fatty liver disease, hepatocellular carcinoma and cholangiocarcinoma (14,15). To date, only few studies investigated the epigenetic changes in autoimmune liver diseases. In primary biliary cholangitis (PBC), hypomethylation of several gene promoters, especially within the X chromosome, has been documented (16-18). Additionally, different expressions of several miRNAs have been reported in PBC and primary sclerosing cholangitis (19-22). In AIH, epigenetic data is even more limited, with only one study reporting significant association of elevated miR21 with the biochemical and histological activity of AIH and decreased miR21 and miR122 in cirrhotic patients (23).

As from the best of our knowledge, DNA $5^{m}C/5^{hm}C$ have not been explored in AIH, we investigated the potential presence of DNA methylation modifications in peripheral B- and T-cells from AIH patients by assessing alterations in DNA methylation through the analysis of global $5^{m}C$ and DNMT1/3A/3B expression as well as alteration in $5^{hm}C$ and TETs transcriptional expression levels. Such analysis was performed at diagnosis and remission. Differences in total $5^{m}C/5^{hm}C$ state between AIH patients at diagnosis and healthy controls (HC) were also assessed by immunohistochemistry (IHC) on paraffin embedded liver sections. Finally, in an attempt to evaluate the methylation alterations in specific CpG sites across the whole genome, we performed epigenome wide association study (EWAS) in CD4(+)-cells from patients and controls using the Illumina HumanMethylation 850K array.

Patients and Methods

Study samples and peripheral mononuclear cells (PBMCs) preparation

PBMCs from 10 AIH patients were isolated from peripheral blood collected at the time of diagnosis (AIH time-point 1; AIH-tp1), by gradient centrifugation (Histopaque-1077, Sigma-Aldrich, St. Louis, MI, USA). PBMCs were then mixed with freezing medium (FBS with 10% DMSO Sigma-Aldrich) and cryopreserved in liquid nitrogen until use.

In eight of these patients, PBMCs were also isolated at a second time-point when they had complete biochemical response under immunosuppression (AIH time-point 2; AIH-tp2). According to the guidelines of the Hellenic Association for the Study of the Liver (5) and our published protocols (24,25), AIH-tp2 patients were receiving at the time of investigation either combination therapy with prednisolone 0.5-1mg/kg/day and mycophenolate mofetil 1.5-2g/day (MMF; n=6) or MMF maintenance monotherapy (n=2). Ten healthy served as HC and 9 PBC patients at diagnosis before treatment initiation served as the disease control group. Patients and controls were age- and sex-matched (Supplementary Table 1).

As in our previous reports (24,25), all biopsies were assessed using the Knodell histologic/activity index score (26) and patients were divided into two groups according to inflammation: minimal-mild and moderate-severe and

according to fibrosis: minimal/mild-moderate and severe fibrosis-cirrhosis. In PBC, the Ludwig staging system was applied (27).

All patients consented to participate in this study. The ethical committee of the General University Hospital of Larissa approved the protocol which conforms to the ethical guidelines of the 1975 Declaration of Helsinki as reflected in a priori approval by the institution's human research committee (21-03-2016/2258).

CD19(+) B- and CD4(+) T-cells isolation

CD19(+) and CD4(+)-lymphocytes were isolated by ROBOSEP^{TM}-S platform (Stemcell Technologies, Vancouver, USA). CD19(+) B- and CD4(+) T-cells were incubated with specific antibodies for magnetic selection using the EasySep Human CD19 Positive Selection Kit II and Human CD4 Negative Selection Kit, respectively (Stemcell Technologies). Purity of the isolated B- and T-cells was assessed by flow cytometry using PE-Cy5-anti-CD19 and FITC-anti-CD3/PE-anti-CD8 antibody (Biolegend Inc., San Diego, CA, USA) on a Coulter FC-500 flow cytometer (Beckman-Coulter, Brea, CA, USA) (Supplementary Figures 1A-1D). A total average of $1x10^6$ CD19(+) and $2x10^6$ CD4(+)-cells were isolated per sample and stored at -80^0 C.

DNA/RNA extraction and quantification

Genomic DNA was extracted from CD19(+) and CD4(+)-cells with QIAamp Blood mini purification kit (Qiagen, Hilden, Germany). Quantification was measured at 260nm in a UV-VIS Nanodrop spectrophotometer (Thermo Fisher Scientific, Waltham, MA, USA). DNA purity was determined by the ratio of 260nm to 280nm absorbance levels. Approximately, 0.5-1μg of genomic DNA was isolated from CD19(+) and 1-3μg from CD4(+)-cells.

Total RNA was isolated using the RNeasy mini kit (Qiagen) and quantification and purity were determined as described above. Approximately 0.5-1.2μg of total RNA was isolated from CD19 (+) and 1-3.2μg from CD4(+)-cells.

Determination of 5^mC and $5^{hm}C$ DNA levels

5^mC and $5^{hm}C$ DNA levels were determined using MethylFlash^{TM} Global DNA Methylation (5-mC) and Hydroxymethylation (5-hmC) ELISA Easy Kit

(EpiGentek, NY, USA), according to the manufacturer's instructions (Supplementary Patients and Methods).

DNMT1, DNMT3A, DNMT3B, TET1, TET2 and TET3 mRNA quantification

One µg of total RNA was reversed transcribed using random hexamer primers and 10 Units of Transcriptor Reverse Transcriptase according to the Transcriptor First Strand cDNA synthesis kit (Roche Diagnostics, Basel, Switzerland) in a 20µl reaction for 10min at 25°C, 60min at 50°C and 5min at 85°C. Quantitative polymerase chain reaction was carried out using FastStart DNA Master SYBR Green I (Roche Diagnostics) in a total volume of 20µl containing 250nM specific forward and reverse primers. Amplification and detection were performed in a Lightcycler^{R} 96 Instrument (Roche Life Sciences, Bavaria, Germany) under the following conditions: 1 cycle at 50°C for 2min and 95°C for 10min and 40 cycles at 95°C for 15sec and 60°C for 1min. The primers used for DNMT3A, DNMT3B, TET1 and TET2 were as previously described (28). For the quantification of human DNMT1, TET3 and Glyceraldehyde-3-Phosphate Dehydrogenase (GAPDH) genes, commercially specific primers were used: DNMT1: Hs00945875_m1, TET3: Hs00896441_m1, GAPDH: Hs02758991_g1 (Thermo Fisher Scientific, Waltham, MA, USA). Human GAPDH mRNA was chosen as internal control and for quantification of gene expression the comparative CT method [2−(ΔCT target −ΔCT calibrator) or 2−ΔΔCT] was used. Validation experiments were carried out in duplicates and each run was completed with a melting curve analysis to confirm the specificity of the amplification and the lack of primer dimmers.

EWAS

Five hundred ng of DNA from CD4(+)-lymphocytes from AIH (10 tp1 and 5 tp2) and 9 HC were bisulfite-converted (Zymo Research, Irvine, California, USA) and DNA methylation was evaluated by hybridising bisulfite-converted DNA to the Human Methylation EPIC array Bead Chip (Diagenode SA, Belgium), which allows the interrogation of over 850000 methylation sites throughout the genome at single-nucleotide resolution (Supplementary Patients and Methods; EWAS). These steps were performed by NXT-DX Company (Gent, Belgium) according to manufacturer's instructions.

Methylation data was provided as β-values: β=M/(M+U), where M was the fluorescent signal of methylation and U the respective signal of the unmethylated probe. The β-values ranged from 0 (no methylation) to 1 (100% methylation). A quality control on the output of the Illumina Infinium EPIC array was performed with the Bioconductor R package, Chip Analysis Methylation Pipeline (ChAMP), according to which no sample had a proportion of failed probes >0.1. After normalisation, potential batch effects were evaluated with the singular value decomposition method, which did not identify any significant source of variations that needed corrections.

Liver immunohistochemistry (IHC)

Paraffin embedded sections from 6 AIH-tp1 patients and 7 HC obtained during cholecystectomy, were investigated. Staining for $5^{m}C$ and $5^{hm}C$ was performed with anti-5-methylcytosine (5-mC) and anti-5-hydroxymethylcytosine (5-hmC) antibodies [Abcam, 33D3 (ab10805) and RM236 (ab214728)]. 5μm liver sections were deparaffinized by immersing the slides in xylene and in concentration decreasing alcohol grades solution. Antigen retrieval was performed in a Tris- EDTA (pH=9) solution at 98°C for 20 min, while endogenous peroxidase activity was blocked by quenching the tissue sections with 3.0% hydrogen peroxide in methanol for 10 minutes. The sections were then washed with 1% donkey serum in PBS-0,4% Triton X-100 (TBST) solution for 5 minutes for permeabilization, followed by incubation with primary antibody (dilution 1/150) in room temperature for 30 minutes. After washing the sections with TBST solution, they were incubated with Linker and Polymer HRP (Ready to use reagent, Envision Flex, Dako) for 15 and 30 minutes, respectively. Finally, sections were incubated with 3,3'-diaminobenzidin (DAB^{+}) and washed with distilled water. Hematoxylin Harris was used for nuclear counterstaining and dehydration was performed in increasing concentration alcohol solutions and xylene. Negative controls consisted of substitution of primary antibody with pre-immune serum.

Immunohistochemical evaluation

Immunostaining was semi-quantitatively evaluated in a blinded fashion regarding any of the histological and clinical characteristics of the patients by

two independent observers. The degree of staining was determined according to its amount and intensity, using a 4-point scoring system, as follows: 0=no staining; 1=positive nuclear staining in less than 20% of cells; 2=21-50% of positive cells; and 3=positive nuclear staining in more than 50% of cells.

Statistical analysis

Analysis was made using the SPSS 20 and GraphPad-Prism 7.0 software. Results were expressed as median (range) and mean±standard deviation. Data were compared with Kruskall-Wallis and Mann-Whitney U-test for the detection of differences between independent samples and Wilcoxon test for paired samples. Pearson coefficient (R) and Spearman's coefficient (r) were used for correlations, where applicable. Two-sided *p*-values <0.05 were considered as statistically significant in 95% confidence interval.

Statistical analysis of the EWAS data was performed with the Bioconductor R package ChAMP (29). After normalization, identification of differentially methylated positions (DMPs) between groups was performed using Benjamini-Hochberg adjusted *p*-value <0.05. Differentially methylated regions (DMRs) between groups, were identified with BumpHunter method and adjusted *p*-value <0.05 (30). Gene set enrichment analysis using GOmeth method was performed on the genes associated with the DMRs to determine potential enriched pathways (31). Finally, in order to identify if differentially methylated genes shared common functional properties between AIH-tp2 and AIH-tp1, we used the Database for Annotation, Visualization and Integrated Discovery (DAVID), which builds clusters of genes with significantly similar ontologies as tested against a complete list of genes in the database (32). Medium stringency was used to yield a broader set of ontological groups.

Results

Global $5^{m}C$ and $5^{hm}C$ in CD19(+) and CD4(+)-cells and their association with clinical, biochemical and serological parameters

Global $5^{m}C$ and $5^{hm}C$ levels in CD4(+) and CD19(+)-cells did not differ between the study groups (Figure 1). In addition, $5^{m}C$ and $5^{hm}C$ levels in AIH-

tp1 and AIH-tp2 patients were not correlated with age, AST, ALT, IgG, ANA and SMA (data not shown). However, $5^{m}C$ levels in CD4(+)-lymphocytes were negatively correlated with disease duration (r=-0.76; p=0.01) in AIH-tp1 patients.

DNMTs and TETs in CD19(+) and CD4(+)-lymphocytes from AIH-tp1 patients

AIH-tp1 patients had significantly lower TET1 mRNA levels in CD19(+) and CD4(+) lymphocytes compared to HC (p=0.03; p=0.01, respectively; Figures 2A, 2B). AIH-tp1 had significantly higher DNMT3A in CD19(+) and CD4(+) lymphocytes compared to PBC (p=0.04; p=0.002, respectively; Figures 2C,2D). No differences of DNMT1, TET2 and TET3 in CD19(+) or CD4(+)-cells were observed between AIH-tp1 and HC or PBC. Of note, PBC had significantly higher DNMT1 and TET3 in CD19(+)-cells compared to HC (p=0.02; p=0.005, respectively; Supplementary Figures 2A,2B). DNMT3B levels were beyond the detection threshold so no further analysis was made.

Effect of immunosuppression on DNMTs and TETs expression in AIH

AIH-tp2 patients had significantly lower DNMT3A mRNA in CD19(+) (p=0.02) and CD4(+)-lymphocytes (p=0.03) compared to AIH-tp1 (Figures 3A,3B). This supports that immunosuppression controls DNMT3A overexpression as DNMT3A levels in AIH-tp2 did not differ from HC, either in CD19(+) or in CD4(+) lymphocytes (Supplementary Figure 3). The mRNA levels of DNMT1 and TETs did not differ between the two groups (data not shown).

Association of DNMTs and TETs mRNA with clinical, biochemical and serological parameters in AIH-tp1 and AIH-tp2 patients

DNMT3A mRNA in CD4(+)- and CD19(+)-cells of AIH-tp1 was negatively correlated with IgG (R=-0.68; p=0.03 and R=-0.57; p=0.08, respectively) (Figures 3C,3D). In contrast, DNMT3A levels in CD4(+)-cells from AIH-tp2 were positively correlated with IgG (r=0.8; p=0.02).

EWAS in CD4(+) lymphocytes from AIH-tp1 patients compared to HC

As DNMT3A and TET1 mRNA variations were more important in CD4(+) as compared to CD19(+) lymphocytes, CD(4+)-cells were further selected to

investigate DMRs, which are more highly associated with disease as compared to a single CpG analysis. To this end we have used the BumpHunter method and have identified 287 CpG motifs corresponding to 29 DMRs between 10 AIH-tp1 and 9 HC (Figure 4A). These DMRs corresponded to unique and annotated genes present on 26 autosomes and 3 on sex chromosomes. Regarding functional genomic distribution, the majority of DMRs (14/29; 48.3%), corresponded to gene promoters and transcription start sites (TSS), while 6/29 (20.7%) corresponded to introns (Figure 4B). Regarding methylation status, 17/29 (58.6%) genes were hypomethylated (Table 1). Interestingly, 7/8 differentially methylated genes located on chromosome 6 are located on the major histocompatibility complex (MHC). Among them, two are encoded by MHC class-II molecules: HLA-DPA1 (hypermethylated, p=0.003.) and HLA-DPB2 (hypomethylated, p=0.01). In addition, the long intergenic non-protein coding RNA 2571 gene (LINC02571), which belongs to the group of long noncoding RNAs (lncRNAs), was retrieved hypermethylated (p=0.02), while the promoter of the tumor necrosis factor (TNF) gene was hypomethylated (p=0.01; Table 1) and ZFP57 was hypermethylated (p=0.02).

One of the most differentially methylated genes (p=0.0002) was the promoter of platelet derived growth factor receptor like gene. Finally, the RhoH gene was found hypermethylated (p=0.01; Table 1).

Using the GOmeth method, no pathways were identified as enriched based on the genes associated with the identified DMR.

EWAS in CD4(+) lymphocytes from AIH-tp1 patients compared to AIH-tp2

Next, we investigated whether methylation of the CpG motifs is affected by immunosupression in CD4(+) lymphocytes from AIH (10 AIH-tp1 and 5 AIH-tp2). In AIH-tp2 and at CpG level, 831 differentially methylated probes (DMPs; 11,2% hypomethylated and 88,2% hypermethylated) were identified compared to AIH-tp1, corresponding to 576 unique and annotated genes (Figure 5A). DMPs functional genomic distribution retrieved an enrichment in intergenic regions at isolated CpG or open sea regions as well as in gene bodies within shores regions present up to 2kb from CpG islands (Figures 5B,5C).

Although GOmeth did not reveal any enriched pathway, DAVID could categorize 376/576 genes in 12 clusters and 38 subgroups (Supplementary Table 2). The main functional annotations over-represented were those classified as “nucleotide-binding kinases”, “metal-binding proteins”, “phospholipid-metabolism”, “motor-proteins”, “membrane-proteins” ($p<0.05$; Supplementary Table 2). Of note, the annotation cluster “immunity”, comprised of genes most of which were hypermethylated in AIH-tp2 (Supplementary Table 3).

To go further in the analysis of immunosuppression on DNA methylation in CD4(+) lymphocytes, the 14 DMRs between AIH-tp1 and AIH-tp2 (Supplementary Table 4) as well as the top 25 differentially methylated genes (among genes with 2 DMPs) were explored (Table 2). DMRs surrounding promoter regions were predominantly retrieved in 9/14 (64.3%) of AIH-tp2 compared to AIH-tp1. Among the key immune genes differentially methylated between AIH-tp2 and AIH-tp1, the activation marker CD86, the miRNA processing enzyme DROSHA and lncRNAs (LINC00211 and LINC01140) were hypermethylated in AIH-tp2 ($p<0.05$; Table 2).

$5^{m}C/5^{hm}C$ staining in liver sections

Finally, representative intense and diffuse nuclear $5^{hm}C$ immunohistochemical staining in the majority of the lymphocytes infiltrating the portal tract of AIH-tp1 cases is shown in Figure 6A. In addition, strong nuclear immunoreaction was observed in the limiting plate hepatocytes and bile duct epithelial cells of AIH-tp1 cases (Supplementary Table 5, Figure 6A). On the contrary, there was absence of positive lymphocytes in the portal tract of control cases, which also showed lack of immunoreactivity in periportal hepatocytes, and weak immunostaining of few bile duct epithelial cells (Supplementary Table 5, Figure 6B).

Hepatocytes of both AIH-tp1 and control cases showed similar nuclear $5^{hm}C$ and $5^{m}C$ immunostaining (Supplementary Table 5 and 6, respectively). $5^{m}C$ staining of liver infiltrating lymphocytes showed no differences in localization and intensity between patients and controls (Supplementary Table 6).

$5^{m}C$ and $5^{hm}C$ immunostaining of Kupffer cells showed slightly reduced scores between AIH and HC (Supplementary Tables 5 and 6). However, the number of cases studied is small to allow further interpretation.

Discussion

To the best of our knowledge, this is the first study to evaluate the DNA methylation status in liver sections and peripheral B- and T-cells from AIH patients. The following points arise from the present investigation: first, altered TET1 and DNMT3A expression characterizes both CD19(+) and CD4(+)-lymphocytes from AIH-tp1 patients compared to HC and PBC; second, after induction of remission, DNMT3A expression is decreased; third, in AIH-tp1 patients, DNMT3A was negatively correlated with IgG, while the opposite was observed in AIH-tp2 patients; forth, although changes in DNMT3A and TET1 expression were not associated with global and major $5^{m}C/5^{hm}C$ changes, using an EWAS approach we found however, differences of DNA methylation of specific genes in CD4(+)-lymphocytes from AIH-tp1 patients compared to HC and AIH-tp2 patients; and fifth, we observed strong nuclear $5^{hm}C$ staining at the histological level of the periportal infiltrating lymphocytes in AIH-tp1 compared to controls. Taken together, these findings suggest that epigenetic modifications may play an important role in AIH pathogenesis and therapeutic response.

TETs are the main enzymes involved in active DNA demethylation associated with the modification and removal of $5^{m}C$. In mice, it has been shown that TETs play important role in mature B-cell antibody production, but also in facilitating the in-vitro differentiation of naïve CD4(+)-cells to T-regulatory cells (T-regs) by demethylating Foxp3 enhancer CNS2, while in-vivo seem to stabilize the expression of Foxp3 in T-regs (33). Therefore, TET deficient phenotypes are characterized by reduced class switch recombination capacity and decreased Foxp3 stability (33). Our findings of decreased transcriptional expression of TET1 in CD19(+)- and CD4(+)-lymphocytes from AIH patients with active disease may reflect the abovementioned immune dysregulation.

In AIH-tp1, DNMT3A expression in CD19(+)- and CD4(+)-lymphocytes was increased compared to PBC. This finding together with the increased DNMT1 and TET3 levels, which characterized CD19(+)-cells of PBC compared to HC, points to a different epigenetic profile between the two diseases. In addition, increased DNMT3A and DNMT1 transcriptional levels have been reported in CD4(+)-lymphocytes from patients with either clinically or serologically active

systemic lupus erythematosus (SLE) (34). In SLE, both methyltransferases were inversely correlated with markers of disease activity such as, C3 complement component and anti-dsDNA antibody (34). Accordingly, we found that DNMT3A levels in active AIH were negatively associated with IgG, a serological marker of AIH activity. This correlation between DNMT3A mRNA levels and IgG may reflect a DNMT3A dependent plasma cell dysregulation, which increases autoantibody production as indicated by the elevated IgG values (35).

Corticosteroids administration has been reported to alter DNMT1 expression in PBMCs from SLE patients, while MMF has also been shown to induce epigenetic changes (36,37). This is in accordance with our findings, as immunosuppression with MMF seems to decrease DNMT3A expression in both CD19(+)- and CD4(+)-lymphocytes. The decrease of DNMT3A in responders compared to active AIH together with its positive correlation with IgG in patients at remission suggests that immunosuppression probably restores the epigenetic deregulations at least in B-cells.

EWAS in CD4(+)-cells showed methylation alterations of specific genes. Actually, DMRs analysis between AIH-tp1 and HC revealed that most DMRs located on gene promoters indicating their potential effect on the expression of implicated genes. However, recent studies have shown that the hyper/hypomethylation of the regions downstream of promoter-TSS are also highly involved in the regulation of gene expression (38).

Methylation changes in CD4(+)-cells affected, between others, HLA-DP genes. The association of AIH with the HLA class-II alleles was retrieved from early studies, and confirmed from recent genome wide association studies (GWAS) (7,8). In this context, HLA-DP polymorphisms can modulate interactions with the invariant chain chaperone, resulting in presentation of both exogenous and endogenous antigens in CD4(+)-cells (39). In addition, ZFP57 gene was found differentially methylated. ZFP57 belongs to the Methyl-CpG Binding Zinc Finger Proteins (a large family of methyl-binding proteins) and is associated with several cellular processes including regulation of gene expression, genomic imprinting, cell signalling and transcriptional repression (40).

LINC02571 gene was also found hypermethylated. Recent evidence indicates that lncRNAs play important roles in controlling the development of diverse immune cells and the mechanisms of immune cell activation (41). Of note, another gene located on MHC class-III, the TNF gene promoter, was found hypomethylated. This finding keeps up with a recent study of Bovensiepen et al (42), who found that TNF gene expression in liver-infiltrating lymphocytes was strongly upregulated and that the proportion of TNF-producing CD4(+)-cells was elevated both in blood and in the liver of AIH patients compared to HC. Among the rest of the genes found hypo/hypermethylated in AIH-tp1, RhoH (promoter hypermethylation) belongs to the Rho family of small GTPases and plays an important role in positive and negative thymic selection, in the functional differentiation of T-cells and in T-cell activation through TCR signalling (43). Interestingly, most of the genes (88%) of CD4(+)-cells were hypermethylated in AIH-tp2 patients, suggesting a shift in methylation profile after achievement of remission, probably towards a less activated state (37). Furthermore, some of these genes such as, ANXA1 and PYCARD are known to play diverse roles in immune responses, especially in the activation of inflammasome (44).

Among the top differentially methylated genes, CD86 encodes CD86/B7.2 molecule, which is a central costimulatory molecule mainly expressed on antigen presenting cells. However, recently it has been shown that CD86 is also expressed in humans on CD4(+)-cells in response to activation, suggesting a functional role of B7 molecules in the regulation of a T-cell response (45). The hypermethylation of CD86 gene in AIH at remission could signify a central role of CD86 molecule in “switch-off” of the immunological response in AIH. Interestingly, SorCS1 promoter was found hypomethylated in AIH at remission. This is in line with the role of the family of Vps10p receptors in the regulation of production and exocytosis of pro-inflammatory cytokines as well as the immune functions of T and NK-cells during adaptive immune responses (46).

In order to explore “in situ’’ modifications of methylation, that might contribute to AIH molecular phenotype and might influence the methylation status of circulating immune cells, we assessed the $5^{m}C$ and $5^{hm}C$ protein expression in paraffin embedded liver sections. Interestingly, the findings confirmed the

results of EWAS since the majority of the lymphocytes infiltrating the portal tract, and the surrounding individual periportal hepatocytes, in AIH-tp1 liver sections, were hypomethylated (stained strongly for $5^{hm}C$) compared to HC. Of note, periportal hepatocytes and biliary duct epithelial cells seemed to follow the same pattern of hypomethylation, pointing towards an altered methylation milieu in the liver of AIH patients. To our knowledge, this is the first report of the $5^{hm}C$ and $5^{m}C$ liver tissue-mapping of AIH. These findings merit further investigation in large scale studies including a large number of liver biopsies, in order to correlate the specific cellular hypomethylation with the pathogenesis and/or the progression of the disease.

Our study has some limitations as the number of patients and controls was limited. However, the fact that we studied epigenetic modifications in pure peripheral B- and T-cells but also in liver sections, increases the reliability of our findings, as epigenetic changes are cell-type specific and studies on mixed cell populations may lead to ambiguous results.

In conclusion, we showed for the first time, that altered expression of DNMT3A and TET1, as well as altered DNA methylation of specific genes characterize immune cells in periphery and at the histological level of AIH patients, supporting the implication of epigenetic modifications in disease pathogenesis. Notably, epigenetic modifications were associated with disease activity and modified by immunosuppression. These findings open new insights in understanding of disease pathophysiology and may lead to novel therapeutic interventions.

Acknowledgements: This research project was supported in part by a research grant from the Hellenic Association for the Study of the Liver (HASL) and the Research Committee of the University of Thessaly (No. 2466). P. Arvaniti was also supported by a research grant for rare diseases by the Federation for the Development of Internal Medicine in Europe (FDIME).

Abbreviations

$5^{hm}C$	5-hydroxymethyl-cytosine
$5^{m}C$	5-methyl-cytosine
AIH	Autoimmune hepatitis
ALT	Alanine aminotransferase
AMA	Antimitochondrial autoantibodies
ANA	Antinuclear autoantibodies
AST	Aspartate aminotransferase
DAVID	Database for Annotation, Visualization and Integrated Discovery
DMPs	Differentially methylated probes
DMRs	Differentially methylated regions
DNMTs	DNA methyl-transferases
EWAS	Epigenome wide association studies
GAPDH	Glyceraldehyde-3-Phosphate Dehydrogenase
GWAS	Genome wide association studies
HC	Health controls
HLA	Human leucocyte antigen
MHC	Major Histocompatibility complex
miRNAs	micro RNAs
MMF	Mycophenolate mofetil
NASH	Non alcoholic steatohepatitis
PBC	Primary biliary cholangitis
PBMCs	Peripheral blood mononuclear cells
SjS	Sjögren's syndrome
SLA	Soluble liver antigen
SLE	Systemic lupus erythematosus
SMA	Smooth muscle cell antibodies
TETs	Ten-eleven translocation deoxygenases
TSS	Transcription start sites
tp1	time point 1
tp2	time point 2
Tregs	T regulatory
TSS	Transcription start site
UTR	Untranslated region

References

1. Hennes EM, Zeniya M, Czaja AJ, Parés A, Dalekos GN, Krawitt EL, et al. Simplified criteria for the diagnosis of autoimmune hepatitis. Hepatology 2008;48:169–76.

2. Gleeson D, Heneghan MA. British Society of Gastroenterology (BSG) guidelines for management of autoimmune hepatitis. Gut 2011;60:1611-29.

3. Zachou K, Muratori P, Koukoulis GK, Granito A, Gatselis N, Fabbri A, et al. Review article: autoimmune hepatitis -- current management and challenges. Aliment Pharmacol Ther 2013;38:887–913.

4. European Association for the Study of the Liver. EASL Clinical Practice Guidelines: Autoimmune hepatitis. J Hepatol 2015;63:971–1004.

5. Dalekos G, Koskinas J, Papatheodoridis GV. Hellenic Association for the Study of the Liver Clinical Practice Guidelines: Autoimmune hepatitis. Ann Gastroenterol 2019;32:1–23.

6. Mack CL, Adams D, Assis DN, Kerkar N, Manns MP, Mayo MJ, et al. Diagnosis and management of autoimmune hepatitis in adults and children: 2019 practice guidance and guidelines from the American Association for the Study of Liver Diseases. Hepatology 2020;72:671-722.

7. Boer YS de, Gerven NMF van, Zwiers A, Verwer BJ, Hoek B van, Erpecum KJ van, et al. Genome-wide association study identifies variants associated with autoimmune hepatitis type 1. Gastroenterology 2014;147:443-52.e5

8. Czaja AJ, Doherty DG, Donaldson PT. Review: Genetic bases of autoimmune hepatitis. Dig Dis Sci 2002;47:2139–50.

9. Czaja AJ. Global disparities and their implications in the occurrence and outcome of autoimmune hepatitis. Dig Dis Sci 2017;62:2277–92.

10. Renaudineau Y, Youinou P. Epigenetics and autoimmunity, with special emphasis on methylation. Keio J Med 2011;60:10–6.

11. Lu Q, Renaudineau Y, Cha S, Ilei G, Brooks WH, Selmi C, et al. Epigenetics in autoimmune disorders: highlights of the 10th Sjögren's syndrome symposium. Autoimmun Rev 2010;9:627–30.

12. Arvaniti P, Le Dantec C, Charras A, Arleevskaya MA, Hedrich CM, Zachou K, et al. Linking genetic variation with epigenetic profiles in Sjögren's syndrome. Clin Immunol 2020;210:108314.

13. Rasmussen KD, Helin K. Role of TET enzymes in DNA methylation, development, and cancer. Genes Dev 2016;30:733–50.

14. Pirola CJ, Gianotti TF, Burgueño AL, Rey-Funes M, Loidl CF, Mallardi P, et al. Epigenetic modification of liver mitochondrial DNA is associated with histological severity of nonalcoholic fatty liver disease. Gut 2013;62:1356–63.

15. Loeffler MA, Hu J, Kirchner M, Wei X, Xiao Y, Albrecht T, et al. miRNA profiling of biliary intraepithelial neoplasia reveals stepwise tumorigenesis in distal cholangiocarcinoma via the miR-451a/ATF2 axis. J Pathol 2020;252:239-51.

16. Selmi C, Cavaciocchi F, Lleo A, Cheroni C, De Francesco R, Lombardi SA, et al. Genome-wide analysis of DNA methylation, copy number variation, and gene expression in monozygotic twins discordant for primary biliary cirrhosis. Front Immunol 2014;5:128.

17. Lleo A, Zhang W, Zhao M, Tan Y, Bernuzzi F, Zhu B, et al. DNA methylation profiling of the X chromosome reveals an aberrant demethylation on CXCR3 promoter in primary biliary cirrhosis. Clin Epigenetics 2015;7:61.

18. Arvaniti P, Zachou K, Lyberopoulou A, Gatselis NK, Brooks WH, Dalekos GN, et al. Epigenetic modifications in generalized autoimmune epithelitis: Sjögren's syndrome and primary biliary cholangitis. Epigenomes 2019;3:15.

19. Tan Y, Pan T, Ye Y, Ge G, Chen L, Wen D, et al. Serum microRNAs as potential biomarkers of primary biliary cirrhosis. PloS One 2014;9:e111424.

20. Rodrigues PM, Perugorria MJ, Santos-Laso A, Bujanda L, Beuers U, Banales JM. Primary biliary cholangitis: A tale of epigenetically-induced secretory failure? J Hepatol 2018;69:1371-1383.

21. Banales JM, Sáez E, Uriz M, Sarvide S, Urribarri AD, Splinter P, et al. Up-regulation of microRNA 506 leads to decreased Cl-/HCO3- anion exchanger 2 expression in biliary epithelium of patients with primary biliary cirrhosis. Hepatology 2012;56:687–97.

22. Tomiyama T, Yang G-X, Zhao M, Zhang W, Tanaka H, Wang J, et al. The modulation of co-stimulatory molecules by circulating exosomes in primary biliary cirrhosis. Cell Mol Immunol 2017;14:276–84.

23. Migita K, Komori A, Kozuru H, Jiuchi Y, Nakamura M, Yasunami M, et al. Circulating microRNA profiles in patients with type-1 autoimmune hepatitis. PloS One 2015;10:e0136908.

24. Zachou K, Gatselis N, Papadamou G, Rigopoulou EI, Dalekos GN. Mycophenolate for the treatment of autoimmune hepatitis: prospective assessment of its efficacy and safety for induction and maintenance of remission in a large cohort of treatment-naïve patients. J Hepatol 2011;55:636–46.

25. Zachou K, Gatselis NK, Arvaniti P, Gabeta S, Rigopoulou EI, Koukoulis GK, et al. A real-world study focused on the long-term efficacy of mycophenolate mofetil as first-line treatment of autoimmune hepatitis. Aliment Pharmacol Ther 2016;43:1035–47.

26. Knodell RG, Ishak KG, Black WC, Chen TS, Craig R, Kaplowitz N, et al. Formulation and application of a numerical scoring system for assessing histological activity in asymptomatic chronic active hepatitis. Hepatology 1981;1:431–5.

27. Ludwig J, Dickson ER, McDonald GS. Staging of chronic nonsuppurative destructive cholangitis (syndrome of primary biliary cirrhosis). Virchows Arch A Pathol Anat Histol 1978;379:103–12.

28. Charras A, Arvaniti P, Le Dantec C, Arleevskaya MI, Zachou K, Dalekos GN, et al. JAK Inhibitors suppress innate epigenetic reprogramming: A promise for patients with Sjögren's syndrome. Clin Rev Allergy Immunol 2020;58:182-193.

29. Morris TJ, Butcher LM, Feber A, Teschendorff AE, Chakravarthy AR, Wojdacz TK, et al. ChAMP: 450k chip analysis methylation pipeline. Bioinforma Oxf Engl 2014;30:428–30.

30. Jaffe AE, Murakami P, Lee H, Leek JT, Fallin MD, Feinberg AP, et al. Bump hunting to identify differentially methylated regions in epigenetic epidemiology studies. Int J Epidemiol 2012;41:200–9.

31. Geeleher P, Hartnett L, Egan LJ, Golden A, Raja Ali RA, Seoighe C. Gene-set analysis is severely biased when applied to genome-wide methylation data. Bioinforma Oxf Engl 2013;29:1851–7.

32. Dennis G, Sherman BT, Hosack DA, Yang J, Gao W, Lane HC, et al. DAVID: Database for annotation, visualization, and integrated discovery. Genome Biol 2003;4:R60.

33. Lio C-WJ, Rao A. TET Enzymes and 5hmC in Adaptive and Innate Immune Systems. Front Immunol 2019;10:210.

34. Balada E, Ordi-Ros J, Serrano-Acedo S, Martinez-Lostao L, Rosa-Leyva M, Vilardell-Tarrés M. Transcript levels of DNA methyltransferases DNMT1, DNMT3A and DNMT3B in CD4+ T cells from patients with systemic lupus erythematosus. Immunology 2008;124:339–47.

35. Barwick BG, Scharer CD, Martinez RJ, Price MJ, Wein AN, Haines RR, et al. B cell activation and plasma cell differentiation are inhibited by de novo DNA methylation. Nat Commun 2018;9:1900.

36. Yang Y, Tang Q, Zhao M, Liang G, Wu H, Li D, et al. The effect of mycophenolic acid on epigenetic modifications in lupus CD4+T cells. Clin Immunol 2015;158:67–76.

37. Peters FS, Peeters AMA, Hofland LJ, Betjes MGH, Boer K, Baan CC. Interferon-gamma DNA methylation is affected by mycophenolic acid but not by tacrolimus after T-cell activation. Front Immunol 2017;8:822.

38. Anastasiadi D, Esteve-Codina A, Piferrer F. Consistent inverse correlation between DNA methylation of the first intron and gene expression across tissues and species. Epigenetics Chromatin 2018;11:37.

39. Anczurowski M, Hirano N. Mechanisms of HLA-DP Antigen processing and presentation revisited. Trends Immunol 2018;39:960–4.

40. Brandt B, Rashidiani S, Bán Á, Rauch TA. DNA methylation-governed gene expression in autoimmune arthritis. Int J Mol Sci 2019;20:5646.

41. Atianand MK, Caffrey DR, Fitzgerald KA. Immunobiology of long noncoding RNAs. Annu Rev Immunol 2017;35:177–98.

42. Bovensiepen CS, Schakat M, Sebode M, Zenouzi R, Hartl J, Peiseler M, Li J et al. TNF-producing Th1 cells are selectively expanded in liver infiltrates of patients with autoimmune hepatitis. J Immunol 2019;203:3148-3156.

43. Dorn T, Kuhn U, Bungartz G, Stiller S, Bauer M, Ellwart J, et al. RhoH is important for positive thymocyte selection and T-cell receptor signaling. Blood 2007;109:2346–55.

44. Man SM, Kanneganti T-D. Regulation of inflammasome activation. Immunol Rev 2015;265:6–21.

45. Trzupek D, Dunstan M, Cutler AJ, Lee M, Godfrey L, Jarvis L, et al. Discovery of CD80 and CD86 as recent activation markers on regulatory T cells by protein-RNA single-cell analysis. Genome Med 2020;12:55.

46. Talbot H, Saada S, Naves T, Gallet P-F, Fauchais A-L, Jauberteau M-O. Regulatory roles of sortilin and sorLA in immune-related processes. Front Pharmacol 2018;9:1507

Table 1: Differentially methylated genes corresponding to 29 DMRs detected in AIH-tp1 patients and healthy controls (HC).

Gene	Chromosome	Description	Location	Methylation difference (AIH-tp1 vs HC)	p value
CAT	11p13	catalase	promoter-TSS	0.59	0.001
EID3	12q23.3	EP300 interacting inhibitor of differentiation 3	promoter-TSS	-0,65	0.007
GOLGA3	12q24.33	golgin A3	intron	-0.65	0.01
HTR2A	13q14.2	5-hydroxytryptamine receptor 2A	Intergenic	-0.64	0.01
RHOJ	14q23.2	ras homolog family member J	5' UTR	-0.56	0.01
ADAM21P	14q24.2	ADA metallopeptidase domain 21 pseudogene 1	intron	12148	0.0002
BISPR	19p13.11	BST2 interferon stimulated positive regulator	promoter-TSS	0.72	0.004
TYW3	1p31.1	tRNA-yW synthesizing protein 3 homolog	promoter-TSS	0.88	0.0004
PM20D1	1q32.1	peptidase M20 domain containing 1	promoter-TSS	-0.58	0.005
WBP2NL	22q13.2	WBP2 N-terminal like	TTS	-0.56	0.01
PAIP2B	2p13.3	poly(A) binding protein interacting protein 2B	Intergenic	-0.47	0.01
MUC-20	3q29	Mucin 20, Cell Surface Associated	intron	-0.69	0.007
RHOH	4p14	ras homolog family member H	promoter-TSS	0.57	0.01
STPG2	4q22.3	sperm tail PG-rich repeat containing 2	promoter-TSS	0.58	0.02
EIF4E	4q23	eukaryotic translation initiation factor 4E	promoter-TSS	-0.69	0.005
VTRNA2-1	5q31.1	vault RNA 2-1	TTS	0.64	0.002
HLA-DPA1	6p21.32	major histocompatibility complex class II	intron	0.58	0.003
HLA-DPB2	6p21.32	major histocompatibility complex class II	intron	-0.56	0.01
LINC02571	6p21.33	long intergenic non-protein coding RNA 2571 (MHC locus)	Intergenic	0.54	0.02
TCF19	6p21.33	transcription factor 19 (MHC locus)	exon	-0.93	0.001

TNF	6p21.33	tumor necrosis factor (MHC locus)	promoter-TSS	-0.49	0.01
HCG4B	6p22.1	HLA complex group 4B (MHC locus)	promoter-TSS	10439	0.008
ZFP57	6p22.1	ZFP57 zinc finger protein (MHC locus)	Intergenic	0.52	0.02
DDX43	6q13	DEAD-box helicase 43	exon	0.56	0.001
PDGFRL	8p22	platelet derived growth factor receptor like	promoter-TSS	-11703	0.0002
LHX6.1	9q33.2	LIM Homeobox 6	intron	-0.65	0.01
CDK16	Xp11.3	cyclin dependent kinase 16	promoter-TSS	-0.68	0.006
TXLNGY	Yq11.222	taxilin gamma pseudogene	promoter-TSS	-0.59	0.01
EIF1AY	Yq11.223	eukaryotic translation initiation factor 1A	promoter-TSS	-0.82	0.001

AIH-tp1, autoimmune hepatitis time-point 1; AIH-tp2, autoimmune hepatitis time-point 2; TSS: transcription start site; Methylation difference between AIH-tp1 and HC: negative value means hypomethylation.

Table 2: Top 25 differentially methylated genes between AIH-tp2 and AIH-tp1 patients.

Gene	Chromo-some	CpG	Methylation difference (AIH-tp2 vs. AIH-tp1)	Description	P value
ANKRD11	16q24.3	cg00169122 cg08423714	0.07 0.06	Ankyrin Repeat Domain 11	0.03 0.04
ATP11A	13q34	cg16628188 cg14354398	-0.025 0.03	ATPase Phospholipid Transporting 11A	0.04 0.05
CARS1	11p15.4	cg09827966 cg04137890	0.03 0.02	Cysteinyl-TRNA Synthetase 1	0.04 0.05
CD86	3q13.33	cg13617155 cg20753131	0.098 0.075	CD86 Molecule	0.04 0.04
COL15A1	9q22.33	cg14259208 cg07251446	-0.028 0.063	Collagen Type XV Alpha 1 Chain	0.04 0.04
DNAH2	17p13.1	cg22573230 cg26524256	0.087 0.02	Dynein Axonemal Heavy Chain 2	0.04 0.04
DPH6	15q14	cg12382372 cg26149924	-0.05 0.08	Diphthamine Biosynthesis 6	0.05 0.05
DROSHA	5p13.3	cg15628639 cg09622076	-0.063 0.015	Drosha Ribonuclease III	0.03 0.05
ENOX1	13q14.11	cg24171628 cg10448831	0.04 0.026	Ecto-NOX Disulfide-Thiol Exchanger 1	0.03 0.04
TAF5/FAM19A5	22q13.32	cg12555819 cg13520744	0.054 0.04	FAM Chemokine Like Family Member 5	0.04 0.05
H6PD	1p36.22	cg09021539 cg13943024	0.046 -0.03	Hexose-6-Phosphate Dehydrogenase/Glucose 1-Dehydrogenase	0.03 0.04
INPP5B	1p34.3	cg01300277 cg23310078	0.063 0.07	Inositol Polyphosphate-5-Phosphatase B	0.03 0.05
LINC00211	2p22.2	cg12176155 cg00832367	0.039 0.019	Long Intergenic Non-Protein Coding RNA 211	0.009 0.04
LINC01140	1p22.3	cg10277282 cg23492309	0.06 0.08	Long Intergenic Non-Protein Coding RNA 1140	0.04 0.04
LMF1	16p13.3	cg10301401 cg03796797	0.019 0.048	Lipase Maturation Factor 1	0.04 0.04
MAGEC2	Xq27.2	cg07549474	0.065	MAGE Family Member E2	0.04
MS4A15	11q12.2	cg27474534 cg01372278	0.017 0.031	Membrane Spanning 4-Domains A15	0.03 0.04
MSRA	8p23.1	cg07122519 cg12712618	0.073 0.023	Methionine Sulfoxide Reductase A	0.03 0.04
PLCB1	20p12.3	cg13788583 cg20272813	0.072 0.052	Phospholipase C Beta 1	0.04 0.03
SNORD115-15	15q11.2	cg20375947 cg10963511	0.076 0.05	Small Nucleolar RNA, C/D Box 115-15	0.04 0.04
ST3GAL4	11q24.2	cg06534890 cg08080418	0.07 0.027	ST3 Beta-GalactosideAlpha-2,3-Sialyltransferase 4	0.02 0.04
ST6GALNAC4	9q34.11	cg17139858 cg20936291	0.04 -0.05	ST6 N-Acetylgalactosaminide Alpha-2,6-Sialyltransferase 4	0.009 0.03
STRA8	7q33	cg25778497 cg15066191	0.044 0.07	Stimulated By Retinoic Acid 8	0.04 0.04
TMEM218	11q24.2	cg27596275 cg19174059	0.029 0.028	Transmembrane Protein 218	0.04 0.04
WDR27	6q27	cg01393964 cg04445182	0.087 0.036	WD Repeat Domain 27	0.04 0.04

AIH-tp1, autoimmune hepatitis time-point 1; AIH-tp2, autoimmune hepatitis time-point 2; CpG, cytosine-phosphate-guanine dinucleotide

Figure 1: No differences were found in $5^{m}C$ **(A and B)** and $5^{hm}C$ levels **(C and D)** in CD19(+) and CD4(+)-cells from AIH-tp1, AIH-tp2, PBC and HC. $5^{m}C$, 5-methylcytosine; $5^{hm}C$, 5-hydroxymethylcytosine; AIH-tp1, autoimmune hepatitis time-point 1; AIH-tp2, autoimmune hepatitis time-point 2; PBC, primary biliary cholangitis; HC, healthy controls; ns, not-significant.

Figure 2: A) CD19(+)-cells from AIH-tp1 characterized by reduced TET1 compared to HC (p=0.03). **B)** CD4(+)-cells from AIH-tp1 characterized by reduced TET1 compared to HC (p=0.01). **C)** Increased DNMT3A was found in CD19(+)-cells from AIH-tp1 compared to PBC (p=0.04). **D)** Increased DNMT3A was found in CD4(+)-cells from AIH-tp1 compared to PBC (p=0.002). TET1, Ten-eleven translocation methylcytosine dioxygenase 1; DNMT3A, DNA methyltransferase 3A; AIH-tp1, autoimmune hepatitis time-point 1; AIH-tp2, autoimmune hepatitis time-point 2; PBC, primary biliary cholangitis; HC, healthy controls.

Figure 3: CD19(+) and CD4(+)-cells after complete remission (AIH-tp2) characterized by decreased DNMT3A mRNA levels (logarithmic scale) compared to AIH-tp1 (**A**; p=0.02 and **B**; p=0.03). **C)** DNMT3A in CD4(+)-cells was negatively correlated with IgG in AIH-tp1 (R=-0.68, p=0.03). **D)** A negative trend was observed between DNMT3A and IgG in CD19(+)-cells from AIH-tp1 (R=-0,57, p=0.08). DNMT3A, DNA methyltransferase 3A; AIH-tp1, autoimmune hepatitis time-point 1; AIH-tp2, autoimmune hepatitis time-point 2.

Figure 4: A) Heatmap of significant CpGs corresponding to 29 DMRs detected between AIH-tp1 and HC (C1-C9: HC, A1-A10: AIH-tp1). **B)** Genomic distribution of 29 DMRs. AIH-tp1, autoimmune hepatitis time-point 1; CpGs, cytosine-phosphate-guanine dinucleotides; DMRs, differentially methylated regions; TSS: transcription start sites, IGR: intergenic regions, 5´UTR: 5´untranslated region; Hypo, hypomethylated; Hyper, hypermethylated.

Figure 5: A) Heatmap of significant CpGs corresponding to 831 DMPs detected between AIH-tp2 (n=5) and AIH-tp1 (n=10) (R1-5: AIH-tp2, A1-10: AIH-tp1). **B)** Genomic distribution of significant DMPs. DMPs are enriched in open sea regions and shores. **C)** Most DMPs are located on gene bodies and IGR. AIH-tp1, autoimmune hepatitis time-point 1; AIH-tp2, autoimmune hepatitis time-point 2; CpGs, cytosine-phosphate-guanine dinucleotides; DMPs, differentially methylated probes; TSS, transcription start sites; IGR, intergenic regions; 5´UTR, 5´untranslated region; 3´UTR, 3´untranslated region; hyper, Hypermethylated; Hypo, hypomethylated.

Figure 6: $5^{hm}C$ immunostaining, original magnification X200. **A)** AIH-tp1: $5^{hm}C$ immunostaining of liver tissue sections shows strong nuclear positivity in the majority of the lymphocytes infiltrating the portal tract (red arrow). Portal inflammatory infiltrate disrupts limiting plate and surrounds individual hepatocytes. The latter show nuclear immunoreaction as well (black arrow). The bile duct epithelial cells show strong immunoexpression (arrowlead). **B)** Controls: $5^{hm}C$ staining shows absence of positive lymphocytes in the portal tract. Note the absence of immunoreactivity in periportal hepatocytes. In addition, a few bile duct epithelial cells show a weaker positive immunoreaction than in AIH. $5^{hm}C$, 5-hydroxymethylcytosine; AIH-tp1, autoimmune hepatitis time-point 1.

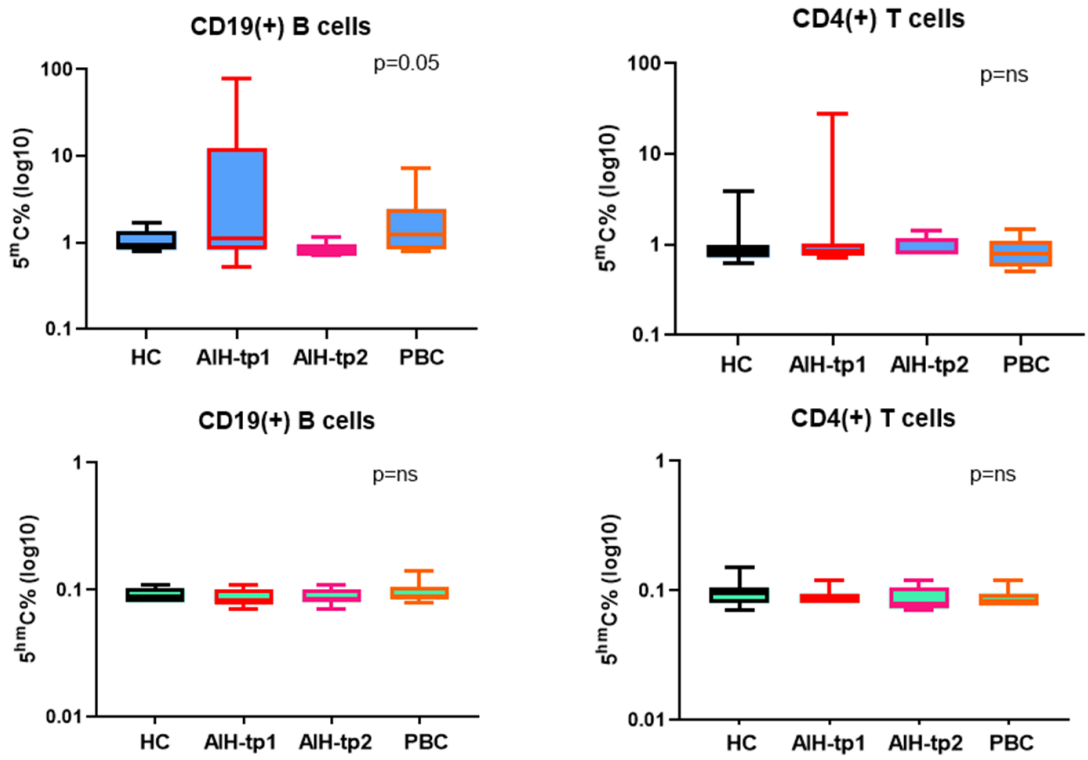

Figure 1

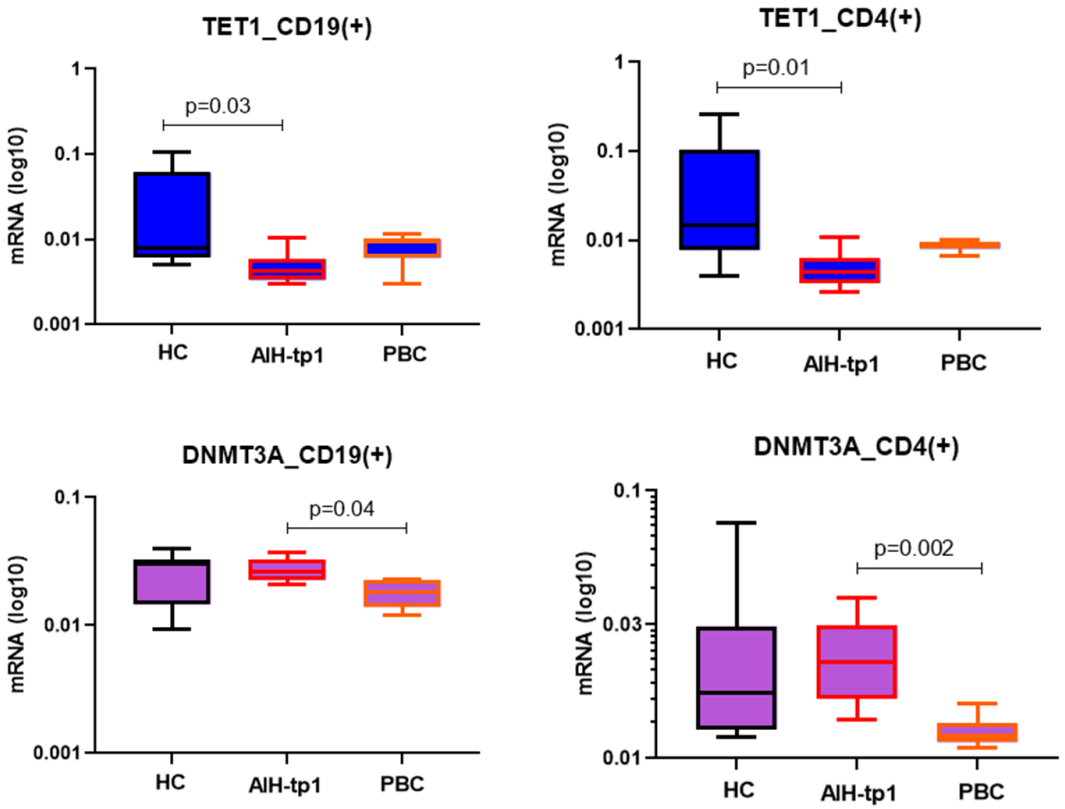

Figure 2

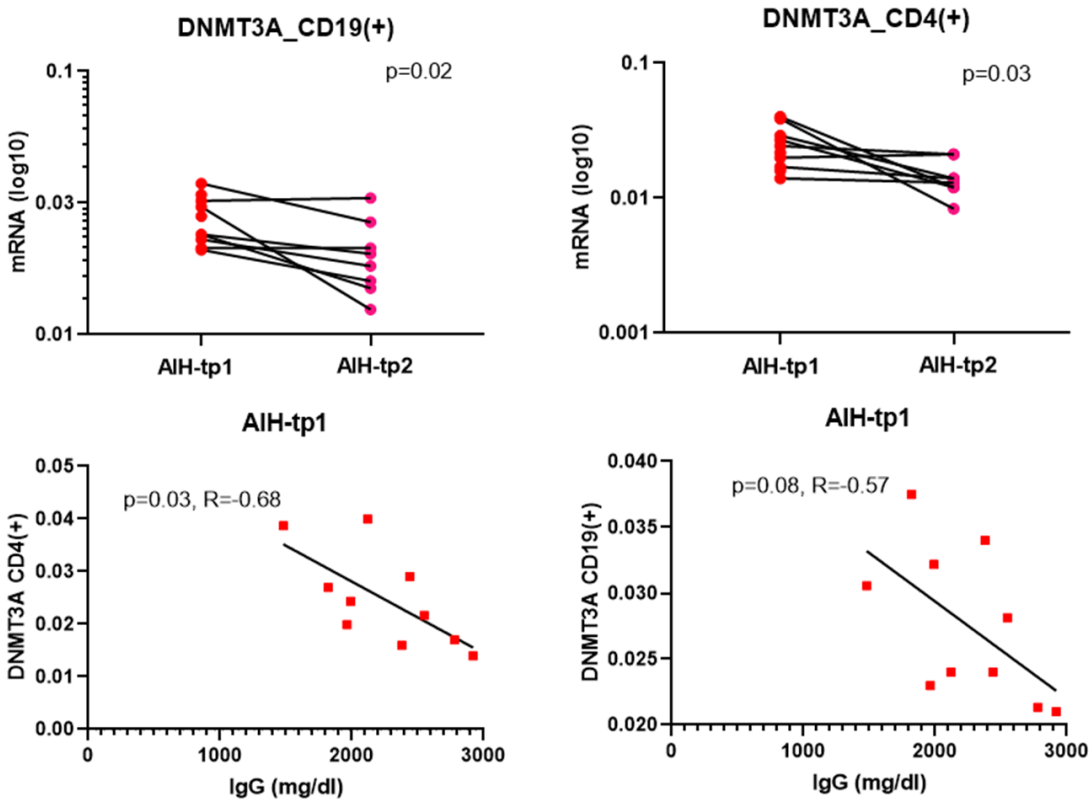

Figure 3

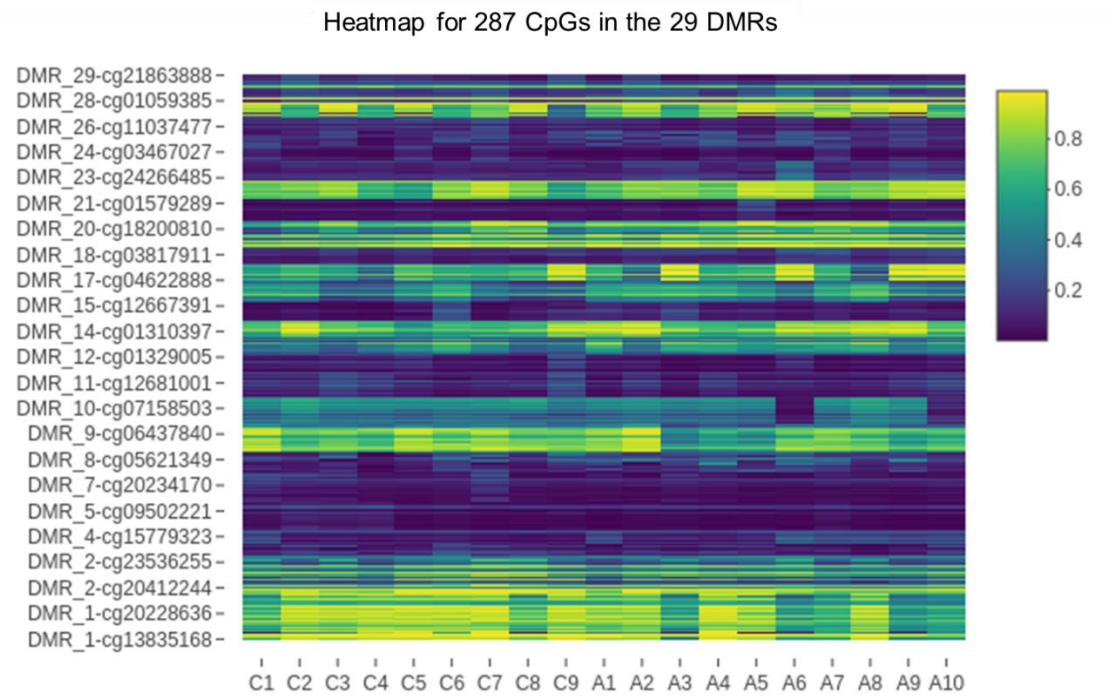

Figure 4A

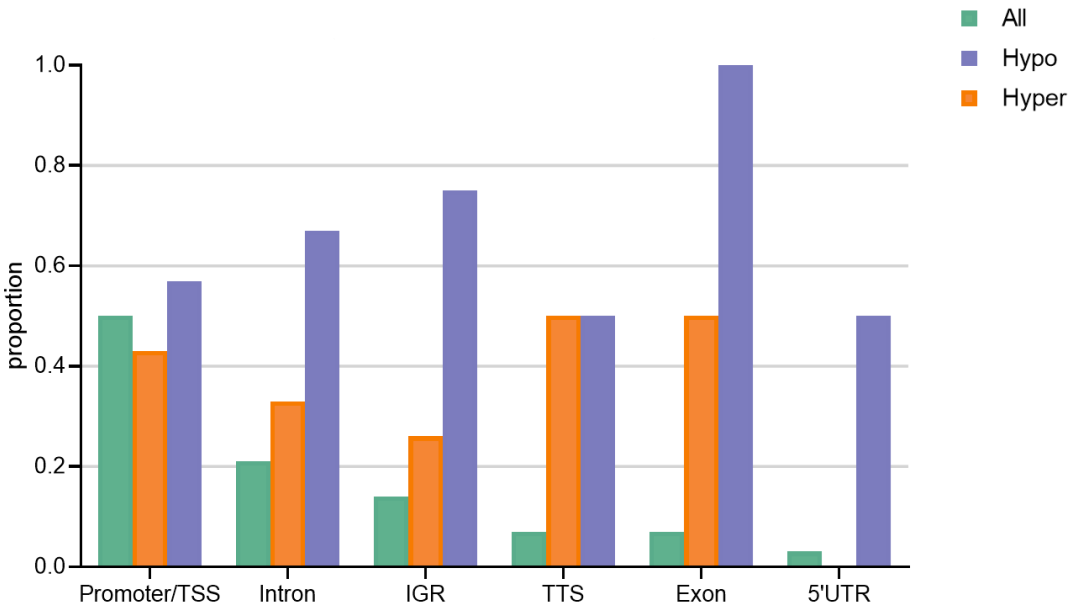

Figure 4B

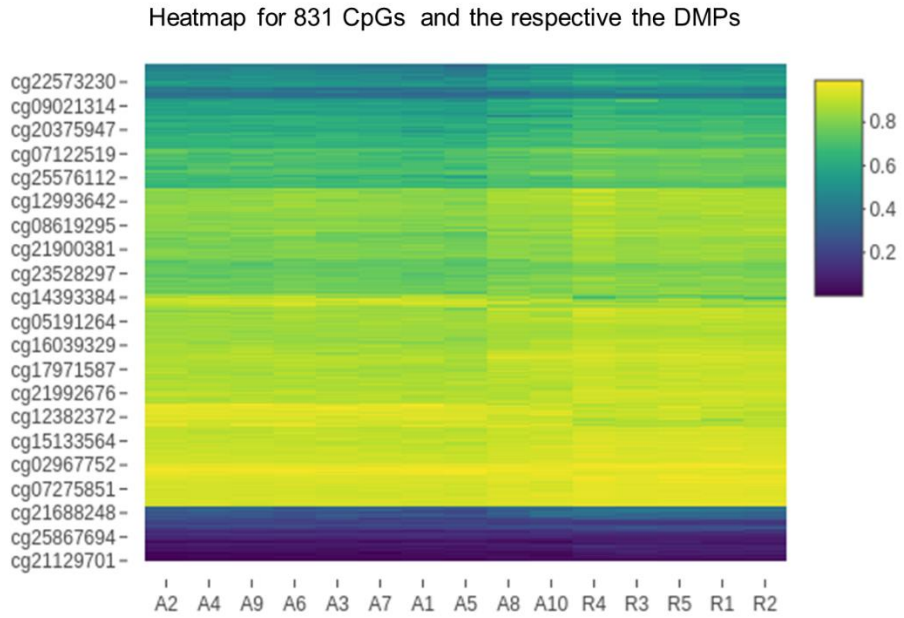

Figure 5A

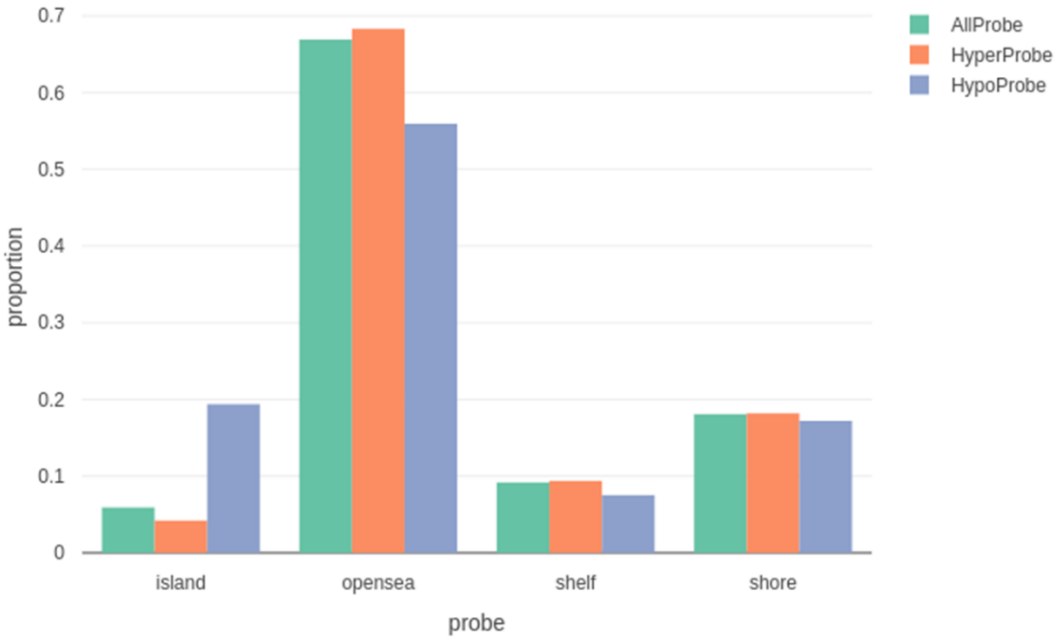

Figure 5B

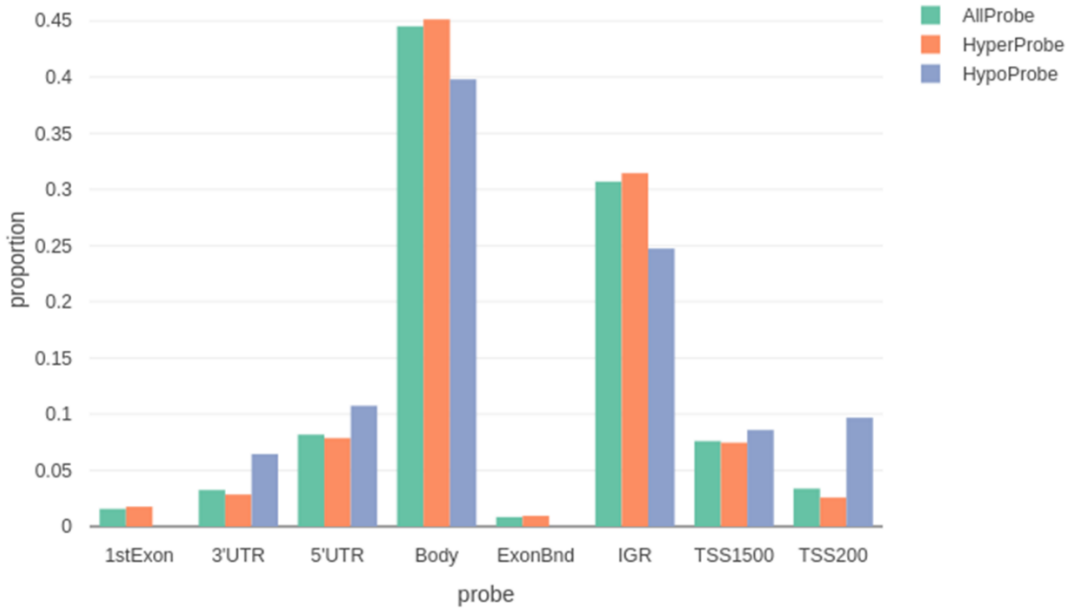

Figure 5C

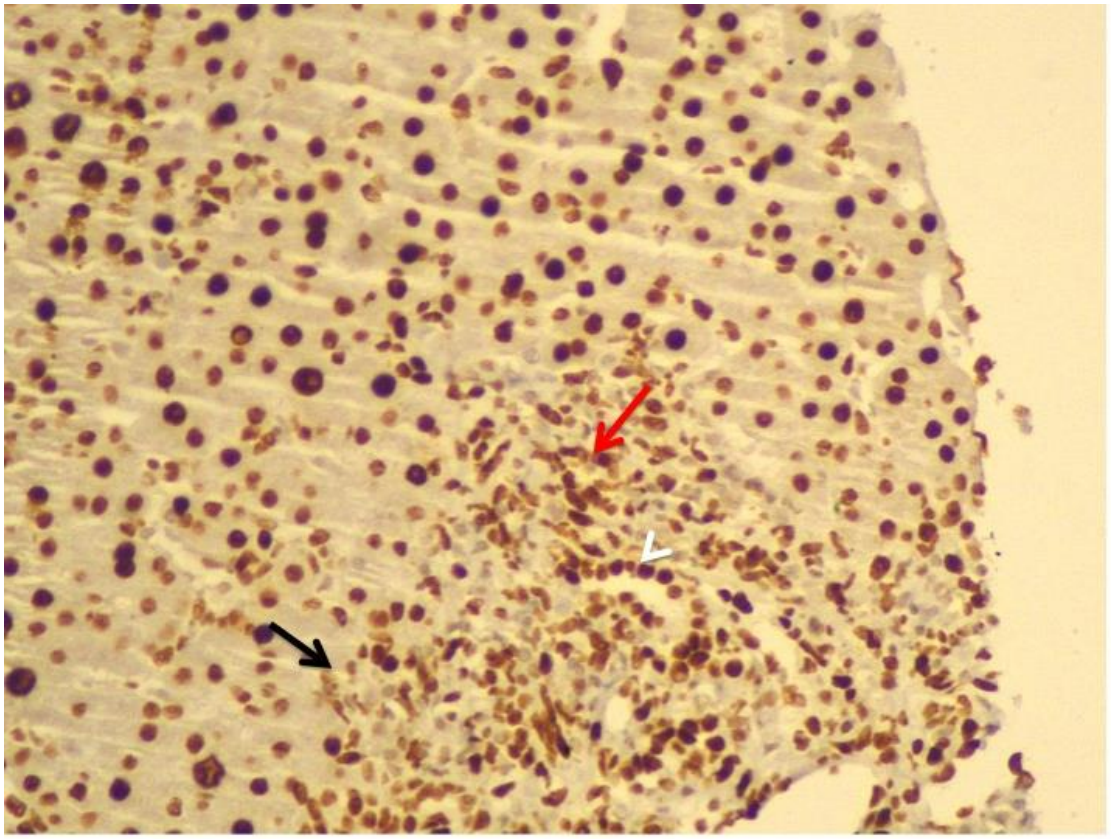

Figure 6A

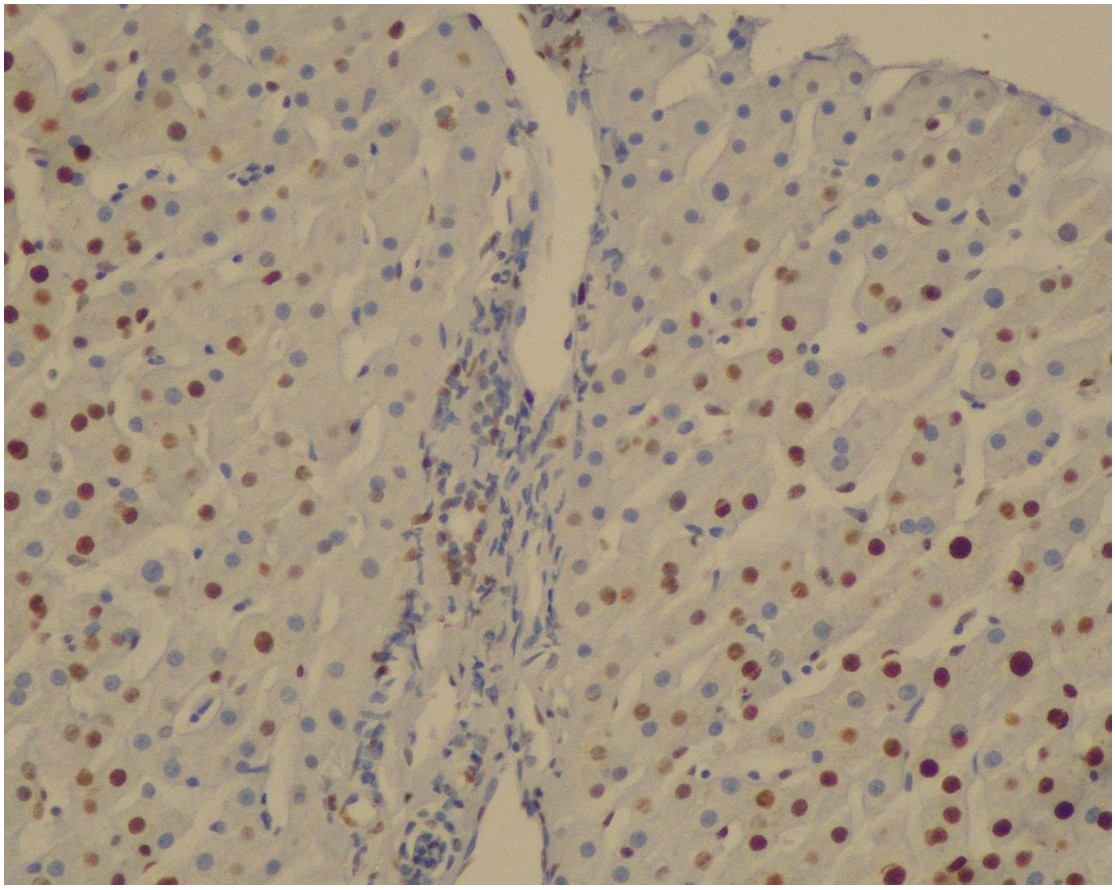

Figure 6B